Electronic spin-fluctuation theory of finite-temperature cluster magnetism: Size and environment dependence in Fe_N

R. Garibay-Alonso,[1] J. Dorantes-Dávila,[2] and G. M. Pastor[3]
[1]*Facultad de Ciencias Físico Matemáticas, Universidad Autónoma de Coahuila, CU Camporredondo, 25000 Saltillo, Mexico*
[2]*Instituto de Física, Universidad Autónoma de San Luis Potosí, Alvaro Obregón 64, 78000 San Luis Potosí, Mexico*
[3]*Institut für Theoretische Physik, Universität Kassel, Heinrich Plett Straße 40, 34132 Kassel, Germany*
(Received 30 October 2008; revised manuscript received 15 January 2009; published 3 April 2009)

The temperature dependence of the magnetic properties of Fe_N clusters ($N \leq 24$) are determined in the framework of a functional-integral itinerant-electron theory. For each exchange-field configuration $\vec{\xi}$, the electronic structure is calculated by using a realistic *d*-band Hamiltonian and a real-space recursive expansion of the local Green's functions. The statistical averages over all $\vec{\xi}$ are performed by implementing a parallel tempering exchange Monte Carlo method. Results are given for the average magnetic moment per atom $\bar{\mu}_N$, local magnetic moments μ_l at different atoms l within the cluster, and interatomic spin-correlation functions γ_{lk} as a function of temperature T. A remarkable dependence of $\bar{\mu}_N(T)$ on size and structure is observed that reflects the importance of the electronic structure to the cluster spin excitations. The correlation between local atomic environment and finite T magnetism is analyzed in some detail by means of the spin-correlation functions. The role of bond-length relaxations on the temperature dependent properties is quantified. An interpretation of our electronic results in terms of Ising or Heisenberg models of localized magnetism reveals a strong dependence of the effective interatomic exchange couplings J_{lk} on size and local coordination number, which defies straightforward transferability and easy generalizations.

DOI: 10.1103/PhysRevB.79.134401 PACS number(s): 75.75.+a, 36.40.Cg, 75.10.Lp

I. INTRODUCTION

The magnetism of small clusters, nanoparticles, and nanostructures are presently the subject of a very intense research activity that is driven by strong fundamental and technological interests. Transition-metal (TM) clusters in particular have been investigated by means of a variety of experimental techniques originally developed in other disciplines such as molecular, surface, and solid-state physics.[1–16] From Stern-Gerlach (SG) deflection measurements on size-selected cluster beams it has been possible to determine the average magnetization per atom $\bar{\mu}_N(T)$ of isolated clusters as a function of the nozzle temperature T. Remarkable temperature dependences of $\bar{\mu}_N$ have been reported for the different magnetic $3d$ TMs.[4–7,14] For example, in Ni_N the measurements show that the magnetization curves are qualitatively similar to the bulk, except for an important finite-size broadening of the transition around the cluster "Curie" temperature T_C.[5,7] Experiments on Co_N show that $\bar{\mu}_N(T)$ is about $0.1-0.5\mu_B$ larger than the bulk magnetization $M(T)$ for $50 \leq N \leq 600$ and $100\ \text{K} \leq T \leq 1000\ \text{K}$.[5,14] Moreover, at low temperatures, $100\ \text{K} \leq T \leq 500\ \text{K}$, the magnetization per atom is found to increase slightly with T. This is an unusual effect that is not observed in the solid. In Fe clusters the temperature dependence derived from experiment is qualitatively different from that of Ni or Co clusters. For $250 \leq N \leq 600$ one observes a rapid, almost linear decrease of $\bar{\mu}_N(T)$ with increasing T ($T \leq 500-600\ \text{K}$). For $T \geq 300\ \text{K}$, $\bar{\mu}_N(T)$ is significantly smaller than the bulk $M(T)$, even though at $T=0$ it was larger [$T_C(\text{Fe-bulk})=1043\ \text{K}$]. As the cluster size increases ($250 \leq N \leq 600$) $\bar{\mu}_N(T)$ decreases further making the difference between cluster and bulk magnetizations even larger.[5] This trend is expected to change for larger Fe clusters, although no experimental evidence seems to be available so far.

From the point of view of theory, mean-field electronic calculations of ground-state properties have been quite successful in predicting a large variety of experimental results on the magnetic behavior of clusters at low temperatures.[17–24] This includes in particular the determination of average magnetic moments per atom,[18–21] the spin and orbital contributions,[22] the magnetic order within the cluster, the magnetic anisotropy energies,[23] etc. In contrast, very little is still known about cluster magnetism at finite temperatures in the framework of an electronic theory.[25,26] This is quite remarkable since a correct description of the temperature dependence of the magnetic properties is crucial for understanding the physics of the underlying many-body problem as well as for controlling the behavior of magnetic clusters in view of technological applications.

One of the major current challenges for theory is to understand how the stability of the magnetic order within nanostructures depends on the size and dimensionality of the system. Simple trends in the size dependence of finite-temperature properties—for example, the cluster "Curie" temperature $T_C(N)$, which measures the energy required to destroy the spin correlations within the cluster— seem difficult to infer *a priori*. On the one side, taking into account the enhancement of the local magnetic moments μ_l^0 at $T=0$ and of the *d*-level exchange splittings $\Delta\varepsilon_{Xl}^d = \varepsilon_{l\downarrow}^d - \varepsilon_{l\uparrow}^d$, one could expect that $T_C(N)$ should be larger and that the ferromagnetic (FM) order should be more stable in small clusters than in the bulk. However, on the other side, the local coordination numbers are smaller at the cluster surface and therefore it should be energetically easier to disorder the local magnetic moments in a cluster by flipping or canting them. If the latter effect dominates, $T_C(N)$ should decrease with decreasing N. In addition, the changes or fluctuations of the cluster structure may also affect significantly the temperature dependence

of the magnetization,[27,28] in particular for systems such as Fe_N and Rh_N which show a remarkable structural dependence of the magnetic properties already at $T=0$.[19,29]

The strong sensitivity of the d-electron properties on the local environment of the atoms suggests that reliable conclusions on cluster magnetism at finite T must be based on an electronic theory that takes into account not only the fluctuations of the magnetic degrees of freedom but also the itinerant character of the d states. In particular one would like that the theoretical description of finite T properties recovers properly the ground-state limit and its well-known diversity of behaviors as a function of size, structure, bond length, etc. Only in this way one may hope to be able to tackle more complex phenomena such as the temperature dependence of orbital moments and magnetic anisotropy. Simple localized-spin models, for example, based on the Heisenberg or Ising model, are not expected to be very predictive, at least until they incorporate the electronic effects responsible for the size dependence of the local magnetic moments and of their exchange couplings. In fact, previous studies of itinerant magnetism in clusters, films, and surfaces have already shown that the effective exchange interactions J_{lm} between nearest-neighbor (NN) moments μ_l and μ_m depend quite strongly on the local environment of atoms l and m.[25,30,31] It is one of the goals of this paper to present a functional-integral theory of cluster magnetism that incorporates the environment dependence of the electronic structure of itinerant d electrons as well as the temperature-induced fluctuations of the spin degrees of freedom. As a first application we perform extensive Monte Carlo (MC) simulations of the finite-temperature magnetic properties of Fe_N clusters in order to reveal their dependence on size, structure, and interatomic distances. Although the sizes considered here are relatively small ($N \leq 24$), qualitative comparisons with cluster experiments, as well as with thin-film and bulk calculations, will be attempted whenever possible.

The remainder of the paper is organized as follows. Section II presents the theoretical background starting from a realistic d-band many-body Hamiltonian and deriving the expressions for the relevant observable properties by using a functional-integral approach to electron correlations and spin fluctuations. The model extends Hubbard and Hasegawa's bulk theory of itinerant magnetism[32–34] in two important respects. First, it incorporates the local environment dependence of the electronic structure, which is central to nanostructures,[35] and, second, it takes into account the collective fluctuations of all the local magnetic moments in the cluster, thus completely removing any of the usual single-site approximations. This is physically important when the size of the cluster is comparable to or smaller than the extent of short-range magnetic correlations.[36] In fact, in this case the temperature dependence of the cluster magnetization is conditioned by the stability of short-range magnetic order which, at least in the bulk, is known to involve a higher energy scale than T_C. In Sec. III the results of our simulation on Fe clusters are presented and discussed. These concern the temperature dependence of the average magnetization per atom, local magnetic moments, and spin-correlation functions. Particular emphasis is given to analyzing the local environment dependence of these properties as a function of size, structure, and interatomic distances. Finally, Sec. IV summarizes the main conclusions, discusses some limitations, and points out some interesting future extensions.

II. THEORY

The magnetic properties of TM clusters at finite temperatures are investigated in the framework of a realistic d-band Hamiltonian,[19]

$$\hat{H} = \hat{H}_0 + \hat{H}_I. \tag{1}$$

The first term

$$\hat{H}_0 = \sum_{l,\alpha,\sigma} \varepsilon_l^0 \hat{n}_{l\alpha\sigma} + \sum_{\substack{l\neq k \\ \alpha,\beta,\sigma}} t_{lk}^{\alpha\beta} \hat{c}_{l\alpha\sigma}^{\dagger} \hat{c}_{k\beta\sigma} \tag{2}$$

describes the single-particle electronic structure of the valence d electrons in the tight-binding approximation.[37] The contribution of s and p electrons is neglected for simplicity, since they are expected to affect both spin directions essentially in the same way. As usual, $\hat{c}_{l\alpha\sigma}^{\dagger}(\hat{c}_{l\alpha\sigma})$ refers to the creation (annihilation) operator of an electron with spin σ at the orbital α of atom l ($\alpha \equiv xy$, yz, zx, x^2-y^2, and $3z^2-r^2$) and $\hat{n}_{l\alpha\sigma}=\hat{c}_{l\alpha\sigma}^{\dagger}\hat{c}_{l\alpha\sigma}$ is the corresponding number operator. ε_l^0 stands for the bare d-orbital energy of the isolated atom and $t_{lk}^{\alpha\beta}$ for the hopping integrals between atoms l and k. The second term,

$$\hat{H}_I = \frac{1}{2} \sum_{\substack{l,\alpha,\beta \\ \sigma,\sigma'}}{}' U_{\sigma\sigma'} \hat{n}_{l\alpha\sigma} \hat{n}_{l\beta\sigma'}, \tag{3}$$

approximates the interactions among the electrons by an intra-atomic Hubbard-type model, where $U_{\sigma\sigma'}$ refers to the Coulomb repulsion between electrons of spin σ and σ'. The prime in the summation indicates that the terms with $\alpha=\beta$ and $\sigma=\sigma'$ are excluded. $U_{\uparrow\downarrow}=U_{\downarrow\uparrow}=F^{(0)}$ is the average direct Coulomb integral and $U_{\uparrow\uparrow}=U_{\downarrow\downarrow}=U_{\uparrow\downarrow}-J$, where $J=(F^{(2)}+F^{(4)})/14$ is the average exchange integral. The $F^{(i)}$ with $i=0,2$, stand for the radial d-electron Coulomb integrals allowed by atomic symmetry.[38] These are obtained by taking the ratios $F^{(0)}/F^{(2)}$ and $F^{(4)}/F^{(2)}$ from atomic calculations[39] and by fitting the value $F^{(2)}$ to reproduce the bulk Fe spin moment at zero temperature. For simplicity we neglect in Eqs. (2) and (3) the dependence of the d-level energies and Coulomb integrals on the orbital α, retaining the dominant spin dependence due to exchange. Notice that Eq. (3) does not respect spin-rotational symmetry, since the exchange terms of the form $\hat{H}_{xy}=-\Sigma_{l,\alpha<\beta}J_{\alpha\beta}(\hat{S}_{l\alpha}^{-}\hat{S}_{l\beta}^{+}+\hat{S}_{l\alpha}^{+}\hat{S}_{l\beta}^{-})$ have been dropped [see also Eq. (4)].[40] Nevertheless, this is not expected to be a serious limitation in the present work, since we are interested in studying the effects of spin fluctuations on broken-symmetry FM ground states.

A. Partition function and derived properties

The finite-temperature magnetic properties of clusters are derived from the canonical partition function $Q=\exp\{-\beta\hat{H}\}$,

where $\hat{H}$ stands for the many-body Hamiltonian given by Eqs. (1)–(3) and $\beta=1/k_BT$. In the case of isolated clusters the temperature T refers to that of the cluster source that defines the macroscopic thermal bath with which the small clusters are in equilibrium before expansion. Thermal average refers then to the ensemble of clusters in the beam. For deposited clusters the temperature is defined by the support. Keeping the number of atoms N and the number of electrons n_d fixed (canonical ensemble) corresponds to the experimental situation found in charge and size-selected beams or at inert (insulating) supports.

The partition function is solved by extending the functional-integral formalism developed by Hubbard and Hasegawa for periodic solids[32–34] to the case of finite systems with arbitrary symmetry.[25,35] To this aim we rewrite the many-body interaction $\hat{H}_I$ as

$$\hat{H}_I=\sum_l\left(\frac{U}{2}\hat{N}_l^2-J\hat{S}_{lz}^2\right), \tag{4}$$

where $\hat{N}_l=\Sigma_{\alpha\sigma}\hat{n}_{l\alpha\sigma}$ is the number operator at atom l, $\hat{S}_{lz}=(1/2)\Sigma_\alpha(\hat{n}_{l\alpha\uparrow}-\hat{n}_{l\alpha\downarrow})$ is the z component of the local spin operator, and $U=(U_{\uparrow\downarrow}+U_{\uparrow\uparrow})/2$. Note that Eq. (4) includes the self-interaction terms $U_{\uparrow\uparrow}\hat{n}_{l\alpha\sigma}^2/2=U_{\uparrow\uparrow}\hat{n}_{l\alpha\sigma}/2$ which are canceled out by redefining the d-energy levels as $\varepsilon_l^0-U_{\uparrow\uparrow}/2$. For the calculation of the canonical partition function Q, the quadratic terms in Eq. (4) are linearized by means of a two-field Hubbard-Stratonovich transformation within the static approximation. Thus, a charge field η_l and an exchange field ξ_l are introduced at each cluster site l, which describe the finite-temperature fluctuations of the d-electron energy levels and local exchange splittings, respectively. Using the notation $\vec{\xi}=(\xi_1,\ldots,\xi_N)$ and $\vec{\eta}=(\eta_1,\ldots,\eta_N)$, Q is given by

$$Q\propto\int d\vec{\eta}d\vec{\xi}\exp\{-\beta F'(\vec{\xi},\vec{\eta})\}, \tag{5}$$

where the free energy F' associated to the exchange fields $\vec{\xi}$ and $\vec{\eta}$ is given by

$$F'(\vec{\xi},\vec{\eta})=\frac{1}{2}\sum_l\left(U\eta_l^2+\frac{J}{2}\xi_l^2\right)-\frac{1}{\beta}ln\{\mathrm{Tr}[\exp\{-\beta\hat{H}'\}]\}. \tag{6}$$

The effective Hamiltonian

$$\hat{H}'=\sum_{l,\alpha,\sigma}\varepsilon'_{l\sigma}\hat{n}_{l\alpha\sigma}+\sum_{\substack{l\neq k\\ \alpha,\beta,\sigma}}t_{lk}^{\alpha\beta}\hat{c}_{l\alpha\sigma}^\dagger\hat{c}_{k\beta\sigma} \tag{7}$$

describes the dynamics of the d electrons as if they were independent particles moving in a random alloy with energy levels $\varepsilon'_{l\sigma}$ given by

$$\varepsilon'_{l\sigma}=\varepsilon_l^0+Ui\eta_l-\sigma\frac{J}{2}\xi_l. \tag{8}$$

The thermodynamic properties of the system are obtained as a statistical average over all possible distributions of the energy levels $\varepsilon'_{l\sigma}$ throughout the cluster. The approach is known as the static approximation, which is exact in the atomic limit ($t_{lm}^{\alpha\beta}=0,\forall l\neq m$) where no fluctuations are present, and in the noninteracting limit ($U_{\sigma\sigma'}=0$).

For $T\to0$ the dominating field configuration $(\vec{\xi}^0,\vec{\eta}^0)$ corresponds to the saddle point in the free energy $F'(\vec{\xi},\vec{\eta})$. This is determined from the self-consistent equations,

$$\left.\frac{\partial F'}{\partial\xi_l}\right|_0=\frac{J}{2}(\xi_l^0-2\langle\hat{S}_{lz}\rangle')=0, \tag{9}$$

and

$$\left.\frac{\partial F'}{\partial\eta_l}\right|_0=U(\eta_l^0+i\langle\hat{N}_l\rangle)=0, \tag{10}$$

where $\langle\cdots\rangle'$ indicates average with respect to the single-particle Hamiltonian H'. Replacing Eqs. (9) and (10) in Eq. (8) yields the known mean-field approximation to the energy levels $\varepsilon'_{l\sigma}$.[19] The present approach provides therefore a proper finite-temperature extension of the self-consistent tight-binding theory developed in Ref. 19 for the ground state.[41]

In this work we are interested in the temperature dependence of the magnetic properties which are dominated by the low lying spin fluctuations. Moreover, $J\ll U$, which implies that the energy involved in local charge fluctuations is much larger than the spin-fluctuation energies. Therefore, it is reasonable to neglect the thermal fluctuations of the charge fields η_l. For each exchange-field configuration $\vec{\xi}$, we set η_l equal to the saddle point of $F'(\vec{\xi},\vec{\eta})$ which is given by $i\bar{\eta}_l=\nu_l=\langle\hat{N}_l\rangle'$. Physically, this means that the charge distribution $\nu_l=\langle\hat{N}_l\rangle'$ is calculated self-consistently for each exchange-field configuration $\vec{\xi}$. Since the ν_l are implicit functions of $\vec{\xi}$, one may write

$$Q\propto\int d\vec{\xi}\exp\{-\beta F'(\vec{\xi})\}, \tag{11}$$

where the free energy,

$$F'(\vec{\xi})=-\frac{1}{2}\sum_l\left(U\nu_l^2-\frac{J}{2}\xi_l^2\right)-\frac{1}{\beta}ln\{\mathrm{Tr}[\exp\{-\beta\hat{H}'\}]\}, \tag{12}$$

associated to $\vec{\xi}$ depends only on the exchange variables ξ_l that describe the relevant fluctuations of the spin degrees of freedom. Notice that $F'(\vec{\xi})$ in Eqs. (11) and (12) is actually a shorthand for $F'[\vec{\xi},\bar{\vec{\eta}}(\vec{\xi})]$ where $\bar{\vec{\eta}}(\vec{\xi})$ refers to the saddle-point value of $\vec{\eta}$ for the exchange configuration $\vec{\xi}$. The integrand in Eq. (11) is proportional to the probability $P(\vec{\xi})=[\exp\{-\beta F'(\vec{\xi})\}]/Q$ of the exchange-field configuration $\vec{\xi}$.

The thermodynamic properties are obtained by averaging over all possible $\vec{\xi}$ with $\exp\{-\beta F'(\vec{\xi})\}$ as weighting factor. For example, the local spin magnetization $m_l=2\langle\hat{S}_{lz}\rangle$ at atom l is given by

$$m_l(T) = \frac{2}{Q}\int d\vec{\xi}\,\exp\left\{\frac{\beta}{2}\sum_l\left(U\nu_l^2 - \frac{J}{2}\xi_l^2\right)\right\}\mathrm{Tr}[\hat{S}_l^z\,\exp\{-\beta\hat{H}'\}], \tag{13}$$

$$= \frac{2}{Q}\int d\vec{\xi}\langle\hat{S}_{lz}\rangle' e^{-\beta F'(\vec{\xi})}, \tag{14}$$

where $\langle\hat{S}_{lz}\rangle'$ is the average spin moment at atom l according to the effective single-particle Hamiltonian $\hat{H}'$, which depends on the fluctuating $\vec{\xi}$. Taking into account that

$$\partial F/\partial\xi_l = \frac{J}{2}(\xi_l - 2\langle\hat{S}_{lz}\rangle'), \tag{15}$$

one may rewrite Eq. (14) as

$$m_l(T) = \frac{1}{Q}\int d\vec{\xi}\xi_l e^{-\beta F'(\vec{\xi})}. \tag{16}$$

Thus, the local magnetization at atom l is equal to the average of the exchange field at the same atom. Equation (16) justifies the intuitive though not quite rigorous association between the fluctuations of the local moment $2\langle\hat{S}_{lz}\rangle$ at atom l and those of the exchange field ξ_l. Notice that in Eqs. (14) and (16) the restriction $\Sigma_l\xi_l \geq 0$ or positive total cluster moment $\Sigma_l\langle\hat{S}_{lz}\rangle' \geq 0$, must be enforced in order to avoid trivially vanishing results for the average magnetization due to time-inversion symmetry. This applies to any finite-system calculation and corresponds to the experimental situation where the cluster moment is aligned along an external magnetic field. We therefore compute the local magnetizations from

$$m_l(T) = \frac{1}{Q}\int d\vec{\xi}\,\mathrm{sgn}\left(\sum_l \xi_l\right)\xi_l e^{-\beta F'(\vec{\xi})}. \tag{17}$$

The cluster magnetization per atom $\bar{m}_N$ is determined by averaging the z component of the total spin operator $\hat{S}_z = \Sigma_l\hat{S}_{lz}$ under the constraint $\langle\hat{S}_z\rangle' \geq 0$. This is given by

$$\bar{m}_N(T) = \frac{2}{N}\langle|\hat{S}_z|\rangle = \frac{1}{N}\sum_l m_l(T), \tag{18}$$

which corresponds to the cluster average of the local magnetizations m_l. The previous definitions of local and average magnetizations are equivalent to the constraint of positive magnetization used in Monte Carlo simulations of phenomenological spin models such as the Ising model.[43] In this way the local magnetizations $m_l(T)$ can be determined for different local environments in analogy to the layer by layer magnetizations in thin films.

An alternative definition of the average magnetic moment per atom is provided by

$$\bar{\mu}_N(T) = \frac{2}{N}\sqrt{\langle\hat{S}_z^2\rangle}, \tag{19}$$

where

$$\langle\hat{S}_z^2\rangle = \frac{1}{Q}\int d\vec{\xi}\langle\hat{S}_z^2\rangle' e^{-\beta F'(\vec{\xi})} \tag{20}$$

denotes the average of the square total spin. Using Eq. (15) one can express $\langle\hat{S}_z^2\rangle$ in terms of the exchange-field averages as[32]

$$4\langle\hat{S}_z^2\rangle = -\frac{2N}{\beta J} + \frac{1}{Q}\int d\vec{\xi}\xi^2 e^{-\beta F'(\vec{\xi})}, \tag{21}$$

where $\xi^2 = (\Sigma_l\xi_l)^2$. The first term in Eq. (21) cancels the trivial contribution to $\langle\xi^2\rangle$ that is present even if H' is independent of $\vec{\xi}$. The magnetic order within the cluster and its stability at finite T are characterized by the correlation functions,

$$\gamma_{lk} = 4\langle\hat{S}_{lz}\hat{S}_{kz}\rangle = -\frac{2}{\beta J}\delta_{lk} + \frac{1}{Q}\int d\vec{\xi}\xi_l\xi_k e^{-\beta F'(\vec{\xi})}, \tag{22}$$

between the magnetic moments at atoms l and k. Notice that $4\langle\hat{S}_z^2\rangle = \Sigma_{lk}\gamma_{lk}$. Positive (negative) values of γ_{lk} for $l \neq k$ indicate ferromagnetic (antiferromagnetic) correlations which tend to enhance (reduce) the total magnetization per atom $\bar{\mu}_N(T)$. The diagonal elements of γ_{lk} are related to the local magnetic moments,

$$\mu_l = 2\sqrt{\langle\hat{S}_{lz}^2\rangle} = \sqrt{\gamma_{ll}}, \tag{23}$$

at atom l. It should be noted that temperature fluctuations in itinerant-electron magnets not only affect the spin-spin correlation functions, for example, by destroying the ground-state FM order in Fe_N, but can also modify the size of the local spin polarizations μ_l. This contrast with localized magnetism where spin and charge degree of freedoms are well separated. In the applications it is interesting to investigate the different temperature scales yielding changes of the various γ_{lk}, in order to infer which local moments fluctuate more or less easily and which are the moments that trigger the breakdown of the cluster magnetic order.

B. Numerical simulations

The calculation of the partition function and derived magnetic properties involves two averages. The first one concerns the electronic degree of freedom of the effective single-particle Hamiltonian $\hat{H}'$, and the second one the functional integration over the spin degrees of freedom. In practice the averages over $\hat{H}'$ are performed by using for simplicity a grand-canonical ensemble with a $\vec{\xi}$-dependent chemical potential that yields the appropriate fixed total number of electron electrons for all $\vec{\xi}$. The average occupation of the eigenstates of $\hat{H}'$ are then given by the Fermi function $f(\varepsilon)$. This is expected to be a good approximation, since the excitations dominating the temperature dependence of the magnetic order in TMs are the low-energy spin fluctuations rather than the higher single-particle Stoner excitations. In addition, we have checked that using a constant chemical potential does not affect the results significantly. The charge distribution and local spin moment for each

exchange-field configuration are then obtained straightforwardly by integrating the local densities of states (DOS) $\rho_{l\alpha\sigma}(\varepsilon)$ of $\hat{H}'$ as

$$\nu_l = \langle \hat{N}_l \rangle' = \int_{-\infty}^{+\infty} \sum_{\alpha\sigma} \rho_{l\alpha\sigma}(\varepsilon) f(\varepsilon) d\varepsilon, \tag{24}$$

and

$$\langle \hat{S}_{lz} \rangle' = \frac{1}{2} \int_{-\infty}^{+\infty} \sum_{\alpha\sigma} \sigma \rho_{l\alpha\sigma}(\varepsilon) f(\varepsilon) d\varepsilon. \tag{25}$$

In the present work the local DOS is computed by using Haydock-Heine-Kelly's recursion method.[44]

In order to determine the relevant magnetic properties of an N-atom cluster we need to evaluate integrals over N exchange fields where each point involves an electronic calculation that is almost as involved as a ground-state one. The integration procedure must be therefore efficient and unbiased. In this context, the simple Metropolis Monte Carlo method[45] has proven to be particularly useful. However, the simple MC simulation schema very often fails or needs far too long ergodicity times, if the energy landscape is complex showing numerous local minima separated by large barriers. As shown in Ref. 25, this is the case for the free energy $F'(\vec{\xi})$ of Fe clusters, since the magnetic states of positive and negative fields are in general separated by significant barriers. Several improvements have been proposed to overcome this difficulty.[46–51] The ergodicity times can be drastically reduced if several simulations are performed at different temperatures in a parallel way, enabling the exchange of configurations between the various temperatures.[51] In the exchange MC method one considers many replicas of the system of interest, each of which is simulated simultaneously and independently at a different temperature using a conventional Metropolis MC algorithm. In addition to the usual local updates of the spin configurations $\vec{\xi}$, one allows the exchange of configurations at nearby temperatures according to a Metropolis criterion taking into account the involved energy difference between the configurations. This introduces additional nonlocal Markov steps by which a simulation at low temperature can escape from local minima. More details of this method, known as parallel tempering or exchange MC, may be found in Ref. 51. In our calculations, the exchanges of magnetic states between nearby temperatures are attempted once every five parallel cycles. A set of 16 temperatures is considered that yields an acceptance rate of about 0.75 for the exchange of magnetic states.

Before presenting the results for the temperature dependent magnetic properties, and in order to estimate the number of MC cycles needed for achieving reliable averages, it is interesting to discuss the quality of the statistical simulations by taking Fe_6 and Fe_{15} clusters as representative examples. The autocorrelation function,

$$q(\tau, T_m) = \frac{1}{N} \sum_l \langle \xi_i(0) \xi_i(\tau) \rangle_{t,m}, \tag{26}$$

is a quantity that measures the relaxation dynamics of MC simulations. More specifically, $\langle \xi_i(0) \xi_i(\tau) \rangle_{t,m}$ measures the time correlation of the ξ_i exchange field at the MC step τ and temperature T_m with respect to the set of initial values $\{\xi_i(0)\}$. In Fig. 1 we show $q(\tau, \beta_m)$ for Fe_6 and Fe_{15} clusters and for three different representative temperatures. T_1 and T_{16} refer to the lowest and highest temperatures considered in the simulation. Notice that for large temperatures ($T > 1000$ K) q decays very fast vanishing for all the considered clusters at $\tau \simeq 300$. However, for lower temperatures q behaves in a different way depending on the cluster. For instance, for Fe_6 at $T \lesssim 1000$ we find that $q(\tau \simeq 500)$ is far from being negligible [see Fig. 1(a)]. In the case of Fe_{15}, and for the same range of the temperatures, q eventually vanishes at $\tau \simeq 1700$. Only for the lowest temperature $T_1 = 300$ K we observe some relatively small oscillations below $\tau \simeq 2000$. In practice q vanishes for about $\tau \simeq 2000$ cycles for all the considered clusters. Therefore, the number of MC cycles used in this work, namely, $\tau \simeq 20\,000$, is large enough to ensure ergodicity in the simulations keeping the computer time within reasonable limits.

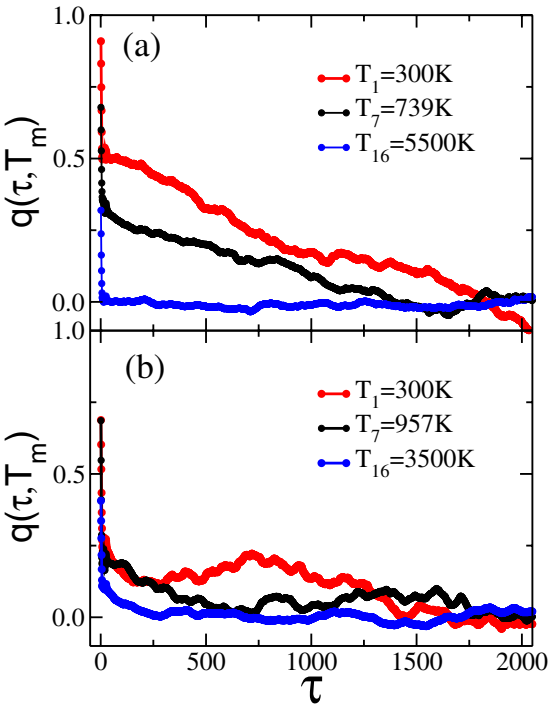

FIG. 1. (Color online) Autocorrelation function $q(\tau, T_m)$ as a function of the Monte Carlo step τ for different temperatures T_m. Results are given for (a) Fe_6 and (b) Fe_{15} clusters and for representative simulations temperatures.

III. RESULTS

In this section we present and discuss results for the temperature dependence of the average magnetizations, $\bar{\mu}_N(T)$ and $\bar{m}_N(T)$, local magnetic moments μ_l, and pair-correlation functions γ_{lk} for Fe_N clusters having $N \leq 24$ atoms. The parameters used for the calculations are the same as in Ref. 19, namely, bulk d-band width $W = 6.0$ eV, direct Coulomb integral $U = 6.0$ eV, and exchange integral $J = 0.73$ eV, which yields the experimental bulk magnetization at $T = 0$, as well

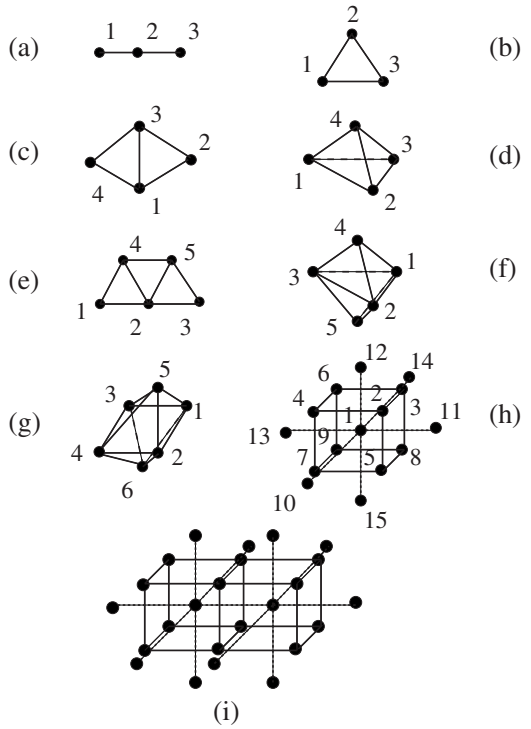

FIG. 2. Illustration of the considered cluster structures of Fe_N clusters ($N \leq 24$). The numbers label the different atomic sites l.

as the well-known enhancement of the ground-state moments as the size is reduced. In Fig. 2 we show the cluster structures considered for the calculations. For simplicity, the NN interatomic distance of bulk bcc Fe is assumed. Bond-length relaxation effects are quantified in Sec. III C for some representative clusters.

A. Average magnetization

In the following we present the results for the average magnetization obtained from Eqs. (18) and (19). It is interesting to compare these two alternative ways since in the former the average corresponds to the experimental situation in which the cluster moment is aligned by an external magnetic field and the later provides the actual contributions of the local magnetic order to the average magnetization.

The results for temperature dependence of the average magnetization $\bar{\mu}_N$ given by Eq. (19) are shown in Fig. 3. Among the general common features of all curves, we observe the low-temperature saturation of $\bar{\mu}_N$ for small clusters $[\bar{\mu}_N(T \to 0) \simeq 3.0\mu_B$ for $N \leq 6]$ and the enhancement of $\bar{\mu}_N(0)$ with respect to the bulk for $N=15$ and 24. In the other extreme, at high temperatures ($T \gtrsim 4000$ K) $\bar{\mu}_N$ is approximately constant as expected for a randomly disordered magnetic state. Notice that the high-temperature values are somewhat smaller than $\bar{\mu}_N(0)/\sqrt{N}$, which would be the result predicted by a simple localized Ising-type model.[52] This reflects a moderate though significant reduction in the local magnetic moments μ_l, which can be ascribed to the delocalized character of the d states. Notice that the high-temperature limit of $\bar{\mu}_N$, as well as of the local moments μ_l to be discussed below, is essentially independent of the details of the electronic structure and of the cluster geometry. It is mainly a statistical local effect. The temperature dependence linking the low and high T limits is not universal, i.e., it depends strongly on the cluster geometry and on the details of the single-particle spectrum. Remarkably, a strong structural dependence of $\bar{\mu}_N(T)$ is found, even in situations where the ground-state moments are saturated and therefore do not depend significantly on structure (e.g., in small clusters). The differences in $\bar{\mu}_N(T)$ are found to be very important in Fe_3 and to lesser extent in Fe_4 and Fe_5 (see Fig. 3). However, notice that at high temperatures, in the disordered local-moment regime, the differences in $\bar{\mu}_N$ or $\bar{m}_N$ among different isomers disappear completely even in cases where the deviations at low and intermediate temperatures are important (e.g., Fe_3 chain and triangle, or Fe_5 bipyramid and trust). This occurs for $T \simeq 2500-3000$ K, where the pair-correlation functions essentially vanish (see below).

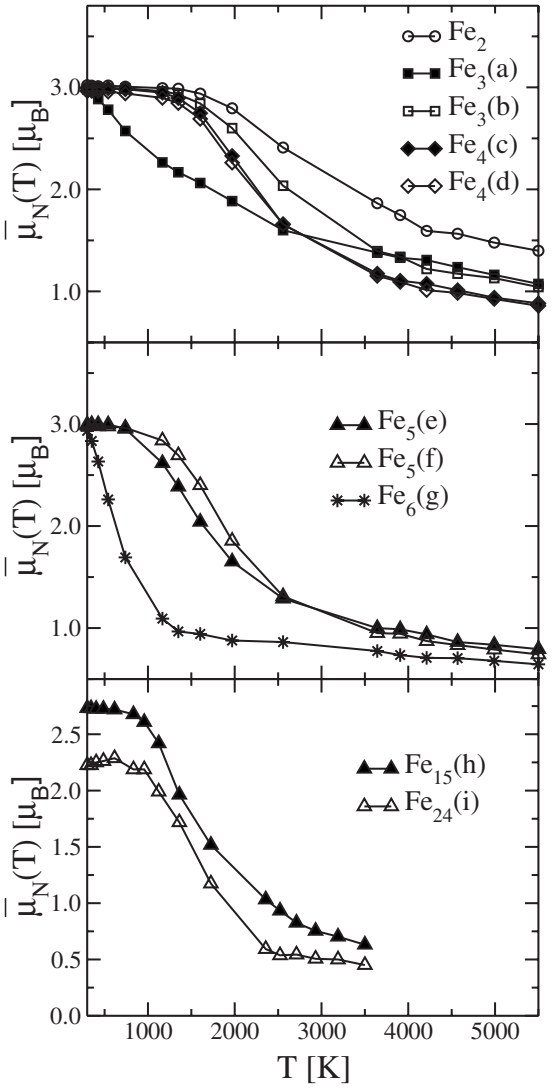

FIG. 3. Temperature dependence of the average magnetic moment per atom $\bar{\mu}_N(T)$ of Fe_N clusters [see Eqs. (19) and (20)]. The labels (a)–(i) refer to the structures shown in Fig. 2.

The stability of cluster ferromagnetism can be quantified by the size-dependent temperature $T_C(N)$ corresponding to

the inflection point in $\bar{\mu}_N(T)$. In the thermodynamic limit $T_C(N)$ should converge to the bulk Curie temperature.[53] However, the physics behind $T_C(N)$ in small clusters should be different than in large nanoparticles and solids. In large systems T_C defines naturally the temperature above which the long-range magnetic order disappears. Nevertheless, a significant degree of short-range magnetic order (SRMO) is observed for $T>T_C$ in the bulk and near surfaces of Fe, Co, and Ni.[30,54,55] Even for large $3d$ TM clusters ($N=50-600$) there is clear experimental evidence for the existence of SRMO above T_C.[4,36] The size of the SRMO domains near T_C has been estimated to be $\nu=15-19$ atoms.[36] For clusters that are smaller than the range of SRMO, it is no longer possible to increase the entropy without destroying the energetically favorable local magnetic correlations. Therefore, the cluster Curie temperature in the limit of $N \lesssim \nu$ should tend to a higher temperature $T_{SR}(N)$ above which thermal fluctuations destroy the short-range correlations between the local magnetic moments, for example, between NN μ_l. This is probably the reason for the relatively large values of $T_C(N)$ derived from our calculations: $T_C(N) \simeq 1500-2500$ K except for linear Fe_3 [$T_C(3) \simeq 750$ K] and square bipyramid Fe_6 [$T_C(6) \simeq 750$ K].

Larger clusters such as Fe_{15} and Fe_{24} have their own special interest since the present nonsaturated spin moments, in contrast to the already discussed smaller ones. Moreover, 15–20 atoms is the typical size of a SRMO domain in Fe. For Fe_{15} the average magnetic moment at very low temperatures is $\bar{\mu}_{15}(0)=2.75\mu_B$ and $\bar{\mu}_{24}(0)=2.25\mu_B$. These values are in agreement with previous works.[19,56] As T increases $\bar{\mu}_N(T)$ remains close to the ground-state magnetization up to $T \simeq 800-1000$ K. Here it starts a rapid decrease, reaching the disordered-local-moment limit for $T \simeq 2500$ K, where $\bar{\mu}_N \simeq \bar{\mu}_N(0)/\sqrt{N}$. The fact that at these temperatures $\bar{\mu}_N$ is close to the average of randomly oriented local moments indicates that these clusters are completely disordered without any significant SRMO being left ($N=15$ and 24 at $T \simeq 2500$ K). This is in agreement with our previous discussion suggesting that $T_C(N) \simeq T_{SR}(N)$ for $N \lesssim \nu$, and is confirmed by more detailed calculations of the correlation functions γ_{lk}. From the inflection point of $\bar{\mu}_N(T)$ we obtain $T_C \simeq 1500$ K which is not far from the bulk value $T_C^{CPA}(\text{bulk})=1600$ K calculated using the same model and the coherent-potential approximation (CPA).[31] Interestingly, in the case of Fe_{24}, we find a slight low-temperature increase of $\bar{\mu}_{24}(T)$ with respect to $\bar{\mu}_{24}(0)$ [see Fig. 3(c)]. This unusual behavior reflects temperature-induced changes in the local electronic structure corresponding to the occupations of higher-spin states. A similar effect has been observed experimentally on large Co clusters.[4,14]

It is interesting to compare the temperature dependence of $\bar{\mu}_N$ for the most compact and highly symmetric clusters ($N=2-5$) since the coordination numbers increase here very fast, almost linear with N. Remarkably, the calculations show that as N increases, $\bar{\mu}_N(T)$ decreases more rapidly with T (see Fig. 3). This means that at $T>0$ the ferromagnetic order becomes comparatively less stable as N and the coordination number z increase. This trend is strictly opposite to the predictions of simple spin models (for instance, the Ising model). In fact, if one would attempt to derive an effective Ising or Heisenberg NN exchange coupling constant J by fitting our electronic calculations, one would conclude that J decreases rapidly with N or z (such as $1/z$ or faster). Obviously, this surprising behavior has to be ascribed to the itinerant character of the d states. As z increases the d-band width increases and with it the relative importance of the kinetic energy as compared to the local exchange energy. This effect appears to be so strong in the case of small Fe clusters that it overcomes the fact that with increasing z the perturbation introduced by the fluctuations of an exchange field ξ_l affect a larger number of atoms and should thus imply a higher excitation energy.

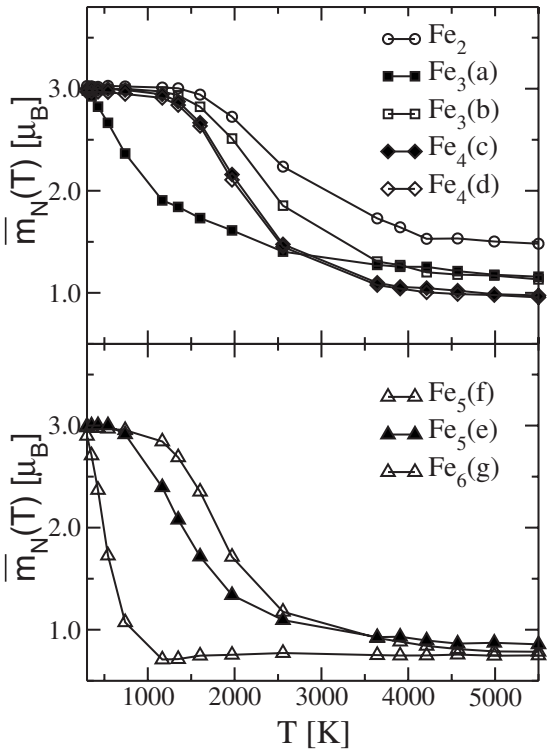

FIG. 4. Temperature dependence of the average magnetization per atom $\bar{m}_N$ of Fe_N clusters [see Eq. (18)]. The labels (a)–(g) refer to the structures shown in Fig. 2.

In Fig. 4 results are given for the average magnetization per atom $\bar{m}_N(T)$ as calculated from Eq. (18). Comparing the results with Fig. 3, one observes that both alternative ways of calculating the average cluster moment yield qualitatively similar magnetization curves in general. Results for larger ferromagnetic clusters (e.g., Fe_{15} and Fe_{24}) confirm this trend. However, for linear Fe_3 and square bipyramid Fe_6, $\bar{m}_N$ decreases with temperature faster than $\bar{\mu}_N$. These differences are probably due to the fact that these clusters develop significant AF-like correlations between second NN moments, as it will be discussed below. The two averages $\bar{\mu}_N$ and $\bar{m}_N$ being qualitatively similar, one may pursue the analysis further from a local perspective by investigating the pair-correlation functions $\gamma_{lk}(T)$, where $\bar{\mu}_N^2=\Sigma_{lk}\gamma_{lk}/N$, and/or the local magnetizations $m_l(T)$, where $\bar{m}_N=\Sigma_l m_l/N$.

B. Local moments and spin correlations

The temperature dependence of the magnetic order within the cluster can be analyzed in more detail by considering the

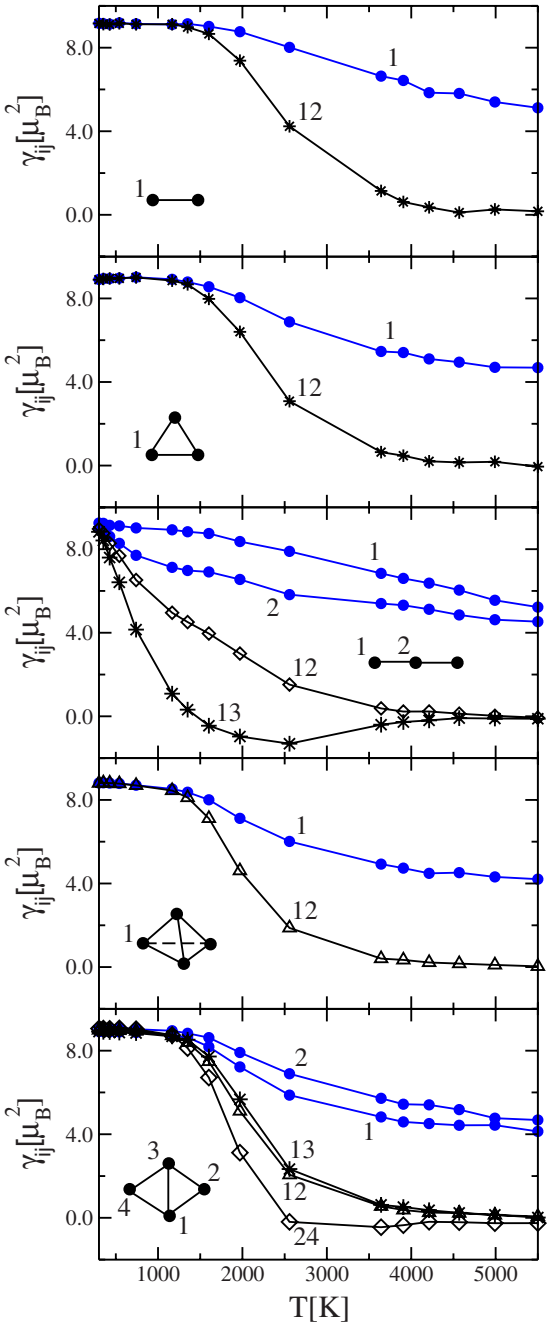

FIG. 5. (Color online) Local magnetic moments μ_l and pair-correlation functions γ_{lk} in small Fe_N clusters having $N \leq 4$ atoms [see Eqs. (22) and (23)]. The numbers refer to the different atoms l or pairs of atoms lk as labeled in the inset figure (or in Fig. 2).

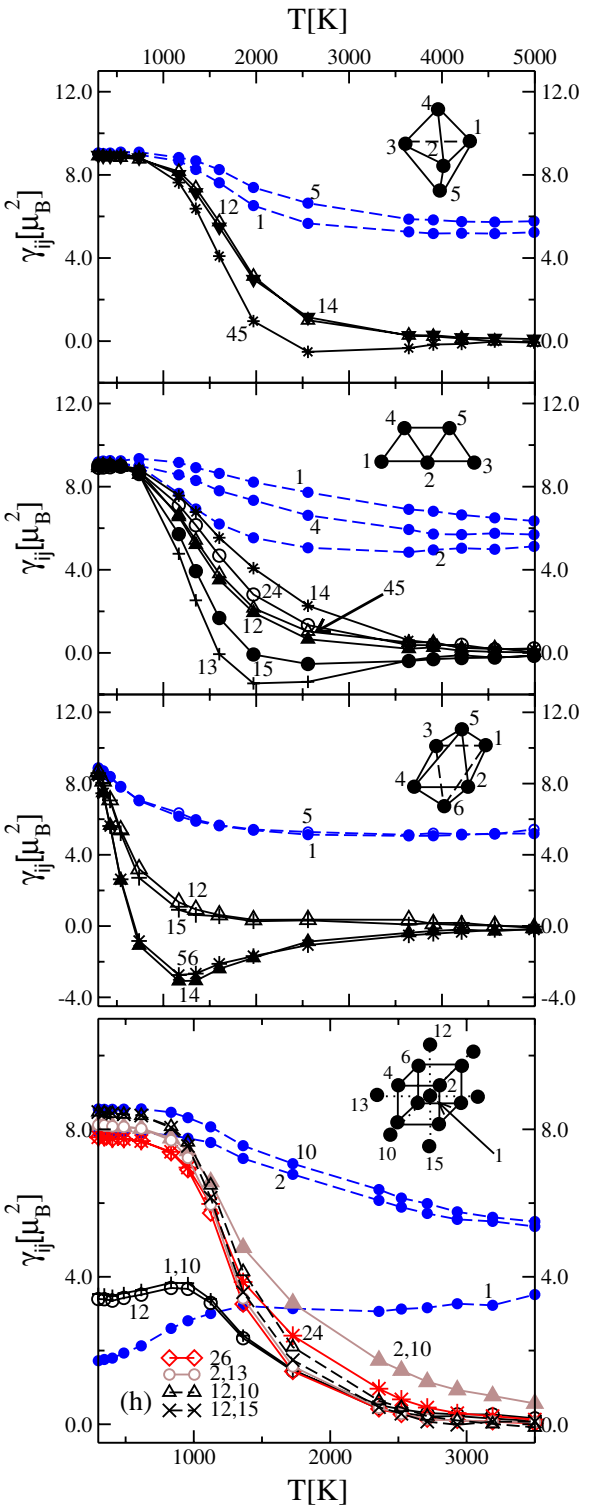

FIG. 6. (Color online) Local magnetic moments μ_l and pair-correlation functions γ_{lk} in Fe_N clusters having $5 \leq N \leq 15$ atoms [see Eqs. (22) and (23)]. The numbers refer to the different atoms l or pairs of atoms lk as labeled in the inset figure or Fig. 2.

spin-correlation functions γ_{lk} [see Eq. (22)]. Comparing the various local moments $\mu_l = \sqrt{\gamma_{ll}}$ and interatomic γ_{lk} allows us to understand the behavior of $\bar{\mu}_N = \sqrt{\Sigma_{lk}\gamma_{lk}}$ from a local perspective and at the same time gain a useful insight on the environment dependence of finite-temperature cluster magnetism. Figures 5 and 6 show our results for the pair-correlation functions and for the square of the local magnetic moments $\mu_l^2 = \gamma_{ll}$ of Fe_N clusters. The suffixes of γ_{lk} correspond to different nonequivalent atoms or pairs of atoms as labeled in Fig. 2. An important feature common to all considered clusters is the remarkable stability of the local moments μ_l^2 at finite temperatures, which are reduced by at most 20%–30% with respect to the ground state, even at the highest considered temperatures. Similar results are found in thin films and bulk Fe.[31] This simplifies the analysis of the

temperature dependent properties, at least to some extent, since in first approximation we may consider that the fluctuating moments have a fixed size. Thus, the magnetic moments preserve a local character despite the fact that the d electrons are delocalized. This is physically quite plausible, since the formation of local moments involves an energy of the order of $J\mu_l^2/4$, that is much larger than the typical spin-fluctuation energies. In addition, the narrowing of the d band in clusters reduces the kinetic or band energy and tends to enhance the localized or directional character of spin fluctuations.[19] The only exception we found to these trends is the moment at the center of a bcc-like Fe_{15} cluster. As will be discussed below, this is related to the fact that the $T=0$ local moments are not saturated at this atom.

The temperature dependence of γ_{12} for Fe_2 and Fe_3 (triangle) follows the behavior of the corresponding $\bar{\mu}_N(T)$ curves as expected for highly symmetric clusters having local moments μ_l that depend weakly on temperature. One observes that the ground-state ferromagnetic coupling is almost fully preserved up to a relatively high temperature $T \simeq 1500$ K. Above this temperature, γ_{12} decreases monotonically, remaining positive and approaching zero ($\gamma_{12} \ll \gamma_{11}$) at approximately $T \simeq 4000$ K. For $T \gtrsim 4000$ K the local moments fluctuate in an uncorrelated way and $\bar{\mu}_N \simeq \mu_l/\sqrt{N}$. As a first example of the role of cluster structure it is interesting to compare the triangle with the linear chain. In linear Fe_3 the ground state is ferromagnetic with saturated moments $\mu_l(0) \simeq 3\mu_B$ and therefore the first NN and second NN correlation functions at $T=0$ are $\gamma_{12}(0) \simeq \gamma_{13}(0) \simeq 9$. However, in this case γ_{12} and γ_{13} decrease very rapidly, almost linearly in T already at very low temperatures [see Fig. 5(c)]. Moreover, γ_{13} changes sign at $T \simeq 1500$ K showing weak antiferromagnetic correlations between second NNs ($\gamma_{13} < 0$). These antiferromagnetic correlations together with the fast decrease in the ferromagnetic NN γ_{12} are responsible for the rapid decrease in $\bar{\mu}_N(T)$ with increasing T. It is interesting to analyze the origin of the second NN antiferromagnetic correlations, since they are also found in other clusters ($N=4-6$) and since they provide some insight into the nature of the dominant spin fluctuations. First of all, one should notice that a negative γ_{13} cannot be understood in terms of uncorrelated local spin fluctuations or unconditional probabilities $p_+(i)$ and $p_-(i)=1-p_+(i)$ of having up and down moments at different sites i. In fact, in this case one would have, using for simplicity a spin-1/2 Ising model, $\gamma_{13}=1-4p_+^2(1-p_+)>0$ for all p_+. Intuitively, in absence of any special correlations, it is clear that positive γ_{12} and γ_{23} should imply a positive γ_{13}. However, if one considers the correlated probabilities $p_1=p_{+++}$, $p_2=p_{++-}=p_{-++}$, and $p_3=p_{+-+}$ of all different configurations on a linear trimer ($\Sigma_i \xi_i \geq 0$), it is easy to show that $\gamma_{13}=1-4p_2$. This is negative provided that p_3 does not increase significantly when p_1 decreases with increasing T[$\gamma_{13}<0 \Leftrightarrow p_2 > (p_1+p_3)/2$]. In other words, $\gamma_{13}<0$ indicates that the dominant spin fluctuations in the linear trimer take place at the extremes of the chain, while spin flips at the central site are much less frequent. As we shall see, a similar analysis applies to larger clusters where the fluctuations at the lowest coordinated sites also dominate over those at the highest coordinated ones (e.g., the rhombus Fe_4, trust Fe_5 and square bipyramid Fe_6).

The pair-correlation functions of the Fe_4 clusters having rhombohedral and tetrahedral geometry are shown in Figs. 5(c) and 5(d). Qualitatively, the tetrahedron resembles the triangle, while the rhombus shows the same main features as the linear trimer with ferromagnetic coupling between first NNs and antiferromagnetic coupling between second NNs above a certain T [see Fig. 5(e) for γ_{13} and γ_{24}, respectively]. As before, the antiferromagnetic correlations result in a faster decrease in the average magnetization with increasing temperature.

Figure 6 shows the pair-correlation functions of Fe_N for $5 \leq N \leq 15$ (see also Fig. 2). For Fe_5 we always find ferromagneticlike correlations between NNs ($\gamma_{ij}>0$), both for the bipyramid [Fig. 6(a)] as for the trust [Fig. 6(b)]. In contrast, the second NNs correlations are antiferromagneticlike above a temperature $T \simeq 1500-2500$ K, depending on the structure and pair of sites. This can be qualitatively understood by analogy with the linear trimer as an indication that the spin fluctuations at the atoms lying at the extremes of the cluster (e.g., $i=4$ and $j=5$ in the bipyramid, and $i=1$ and $j=3$ or 5 in the trust) are much more frequent than the fluctuations of the inner atoms. Notice that negative γ_{ij} are only possible when the average magnetic moments have significantly decreased. Comparing the various γ_{ij} of the two considered Fe_5 isomers, one first of all notes the larger dispersion of the results for the trust, a logical consequence of its lower symmetry. Moreover, one observes that the correlations in the trust decrease in general more rapidly than in the bipyramid. This is consistent with the idea that spin fluctuations are more frequent in weakly coordinated environments. However, for some particular pairs of atoms in the trust (e.g., $i=1$ and $j=4$) the FM correlations are systematically stronger than for any pair of atoms in the bipyramid. In the case of Fe_6 the pair-correlation functions decrease much faster with increasing T than in any of the previously discussed clusters [see Fig. 6(c)]. Moreover, the AF correlations between second NNs are particularly strong here (γ_{14} and $\gamma_{56}<0$). They set in at about $T=700$ K and vanish only above $T=3000$ K. In contrast, the FM-like correlations γ_{12} and γ_{15} are rather weak and disappear above $T=1000$ K. The conjunction of these effects explains the very rapid decrease in $\bar{\mu}_N(T)$ and $\bar{m}_N(T)$ in this cluster (see Figs. 3 and 4).

The characteristic behavior found in very small low-symmetry clusters, i.e., FM correlations for first NNs and AF correlations for second NNs above $T \simeq 1500$, no longer applies to Fe_{15}. In this case all the correlation functions are positive [see, in particular, $\gamma_{1,10}$ and γ_{24} in Fig. 6(c)]. Furthermore, the correlation functions between the pairs involving the central atom $i=1$ (γ_{12} and $\gamma_{1,10}$) as well as the central local moment μ_1 show an unusual temperature dependence. They start from rather small values at $T=0$, and then *increase* with increasing T, as if they were driven by the still strong FM correlations between all the other atoms in the cluster [see Fig. 6(c)]. A change in trend and a decrease of γ_{12} and $\gamma_{1,10}$ is only observed when the fluctuations are so important that the correlations between the atoms $i=2-15$ start to decrease. This effect is most probably due to changes in the local electronic structure with temperature. It suggests that low-energy states with higher spin are occupied at $T>0$. A similar behavior has been found in other clusters

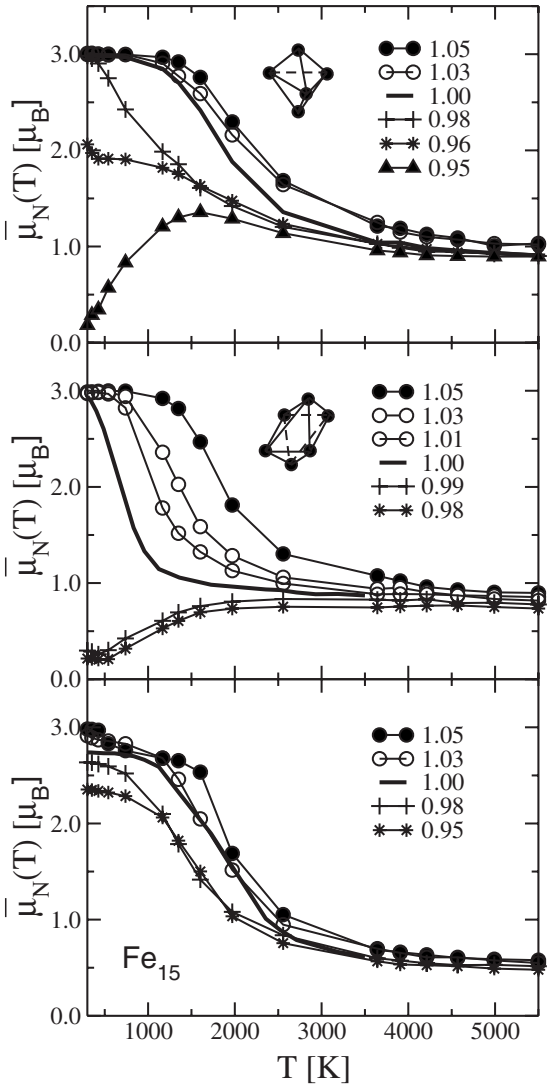

FIG. 7. Bond-length dependence of the magnetization curves $\bar{\mu}_N(T)$ of Fe clusters [see Eqs. (19) and (20)]. Results are given for Fe_5 (triangular bipyramid), Fe_6 (square bipyramid) and Fe_{15} (bcc structure). The numbers indicate the ratio r/r_b between the NN distance r in the cluster and the bulk value r_b.

showing nonsaturated ground-state moments including fully correlated exact-diagonalization studies of Hubbard clusters.[57]

C. Bond-length relaxation effects

The effects of structural relaxations on the magnetic properties of Fe_N clusters have been investigated by varying the NN distance r. In this way, the interplay between kinetic and Coulomb energies can also be explored, since r controls the d-band width and the energy associated to electron delocalization through the distance dependence of the hopping integrals t_{ij}.[58] In this paper, we apply the relation $t_{ij} \sim r^{-5}$ as derived in Ref. 58. As a result the effective coupling constants between the local moments can be manipulated. In Fig. 7 the average magnetization curves $\bar{\mu}_N(T)$ of Fe_5, Fe_6, and Fe_{15} are given for different values of r. Before discussing the temperature dependence of $\bar{\mu}_N(T)$, a few comments on the ground-state moments $\bar{\mu}_N(0)$ are due. For large interatomic distances one obtains saturated $\bar{\mu}_N(0)=3\mu_B$, as expected for a very narrow d-band width. As r decreases, $\bar{\mu}_N(0)$ remains first saturated until r lies below a critical value that depends on size and structure[19] (see Fig. 7). Finally, for very short r the ground-state ferromagnetic order breaks down and $\bar{\mu}_N(0) \rightarrow 0$. Notice that the changes in $\bar{\mu}_N(0)$ with r are very abrupt in small clusters due to the extreme discreteness of the single-particle spectrum.

At finite temperatures one observes very different behaviors depending on the values of r. Let us first consider large distances where the ground-state moments are saturated. For the considered values of r $(r/r_b=1.00-1.05)$ $\bar{\mu}_N(T)$ decreases faster with increasing T when the NN distances are shorter. This is consistent with the trends found in smaller compact clusters, where a larger size or higher coordination number implies a reduction in the cluster Curie temperature. In this range of NN distances magnetism is more stable when the delocalization or band energy is smaller (larger r/r_b). Notice that all the curves start at the same saturated magnetization per atom $\bar{\mu}_N(0)=3\mu_B$. Therefore, the higher $T_C(N)$ cannot be ascribed to an enhancement of the local moments. If one attempts to interpret these results in the framework of an Ising or Heisenberg model, one must conclude that the effective exchange coupling between local moments J_{lk} *increases* with increasing NN distance. Of course, this trend cannot hold in the limit of very large r. One actually observes that the effective J_{lk} goes over a maximum and then decreases if r is further increased. A similar distance dependence of T_C has been found in thin Fe films.[31]

A more interesting temperature dependence of $\bar{\mu}_N(T)$ is found at smaller NN distances, where the $T=0$ moments are not saturated and eventually almost vanish for very small r due to strong d-band broadening. Here, we observe a remarkable enhancement of $\bar{\mu}_N(T)$ with increasing T that indicates, as already mentioned before, the presence of higher-spin states that are populated at finite temperatures. At the same time the local magnetic moments μ_l also increase with T. A similar effect is most probably at the origin of the finite temperature increase in the magnetic moments observed in beam experiments on large Co clusters.[4,14] Notice, moreover, that the simple relation for randomly orientated spins, $\bar{\mu}_N(T > T_C)=\bar{\mu}_N(0)/\sqrt{N}$, is no longer valid in this range of NN distances. These results illustrate very clearly the important interplay of spin fluctuations and electronic structure and the subtle competition between localized and itinerant aspects of d-electron magnetism.[59]

IV. DISCUSSION

The finite-temperature magnetic properties of Fe_N clusters have been determined in the framework of a spin-fluctuation functional-integral theory and a parallel tempering Monte Carlo simulation approach. In this way both the cluster specific electronic structure and the collective fluctuations of the magnetic degrees of freedom at all atoms are treated on the same footing. This is an important improvement with respect to single-site approximations,[25,31–33] which allows us to take

into account and quantify the degree of SRMO in clusters. The study has revealed a variety of new interesting behaviors concerning the dependence of the finite-temperature magnetic properties of clusters as a function of size, structure, and interatomic distances. A remarkable nonmonotonous temperature dependence of the average and local magnetizations has been found. The role of the local atomic environment has been studied by means of the interatomic spin-correlation functions and by varying the NN bond lengths. We have shown that simple Heisenberg or Ising models are not applicable straightforwardly to Fe clusters, since the electronic structure contributions and the itinerant character of the *d* electrons are crucial for determining the magnetic behavior at finite temperatures.

A few comments should be made concerning the possible role of fluctuations of the cluster structure that can be induced by temperature and that could coexist with spin fluctuations of electronic origin considered in the paper. Previous exact-diagonalization studies on the single band Hubbard model have shown that the isomerization energies of magnetic clusters are often comparable to the spin excitation energies.[57] Although we expect the stability of ground-state structures to be higher in realistic *d*-band calculations, it is also true that the contributions of structural fluctuations to the temperature dependence cannot be excluded *a priori*. The effect could be particularly significant in weak unsaturated ferromagnets such as Fe_N, which magnetic moments are known to be very sensitive to structure already for $T=0$.[19] Moreover, as shown in this paper, the stability of ferromagnetism at finite T also depends on cluster geometry. Therefore, the population of low-energy isomers can modify $\bar{\mu}_N(T)$, even if the $T=0$ moments of the excited isomers are nearly the same as for the optimal geometry. In strong ferromagnets the excited isomers are usually quite disordered magnetically when one reaches the temperatures at which they are significantly populated. In this case their contribution to the ensemble average leads to a more rapid decrease in $\bar{\mu}_N(T)$. However, in systems with unsaturated moments it is also conceivable to find excited isomers for which ferromagnetism is stronger and comparatively more stable. In such a situation an increase in $\bar{\mu}_N(T)$ is possible. More detailed investigations taking into account electronic spin fluctuations and structural rearrangement on the same footing are certainly most interesting.

The results discussed in this paper encourage further theoretical developments. The present functional-integral approach to spin fluctuations and the local method of calculations of the electronic structure are well suited to investigate more complex systems with reduced symmetry, such as clusters and nanostructures on surfaces or substrate effects on thin films. In addition, a number of methodological improvements seem worthwhile. The spin-rotational symmetry of the effective Hamiltonian H' could be restored by introducing vector exchange fields $\vec{\xi}_i$ at each atom i. Thus, noncollinear magnetic order and transversal fluctuations of the exchange fields could be taken into account. These are likely to affect the magnetization curves and probably reduce the calculated values of T_C. As already discussed, incorporating structural fluctuations in the statistical average process is also desirable. Another interesting extension concerns the effects of the interactions at interfaces with nonmagnetic substrates, in order to achieve a more realistic comparison with experiments on clusters deposited on surfaces. Last but not least, the model can be readily extended to take into account spin-orbit interactions,[23] and dipole-dipole interactions that are responsible for magnetic anisotropy and for spin reorientation transitions.

ACKNOWLEDGMENTS

This work was supported in part by CONACyT-Mexico (Grant No. 62292) and by the Mexico-Germany exchange program PROALMEX. R.G.A. acknowledges support from PROMEP, Mexico. The authors thank J. Rentería and J. C. Sánchez for technical support. Computer resources provided by Centro Nacional de Supercómputo (IPICyT, Mexico) are gratefully acknowledged.

[1] D. M. Cox, D. J. Trevor, R. L. Whetten, E. A. Rohlfing, and A. Kaldor, Phys. Rev. B **32**, 7290 (1985).
[2] W. A. de Heer, P. Milani, and A. Châtelain, Phys. Rev. Lett. **65**, 488 (1990).
[3] J. P. Bucher, D. C. Douglass, and L. A. Bloomfield, Phys. Rev. Lett. **66**, 3052 (1991); D. C. Douglass, A. J. Cox, J. P. Bucher, and L. A. Bloomfield, Phys. Rev. B **47**, 12874 (1993); D. C. Douglass, J. P. Bucher, and L. A. Bloomfield, *ibid.* **45**, 6341 (1992).
[4] I. M. L. Billas, J. A. Becker, A. Châtelain, and W. A. de Heer, Phys. Rev. Lett. **71**, 4067 (1993).
[5] I. M. L. Billas, A. Châtelain, and W. A. de Heer, Science **265**, 1682 (1994).
[6] D. Gerion, A. Hirt, I. M. L. Billas, A. Châtelain, and W. A. de Heer, Phys. Rev. B **62**, 7491 (2000).
[7] S. E. Apsel, J. W. Emmert, J. Deng, and L. A. Bloomfield, Phys. Rev. Lett. **76**, 1441 (1996).
[8] M. B. Knickelbein, J. Chem. Phys. **115**, 1983 (2001); Phys. Rev. B **75**, 014401 (2007).
[9] C. Binns, Surf. Sci. Rep. **44**, 1 (2001).
[10] D. Zitoun, M. Respaud, M.-C. Fromen, M. J. Casanove, P. Lecante, C. Amiens, and B. Chaudret, Phys. Rev. Lett. **89**, 037203 (2002).
[11] J. T. Lau, A. Föhlisch, R. Nietubyc, M. Reif, and W. Wurth, Phys. Rev. Lett. **89**, 057201 (2002).
[12] P. Gambardella, S. Rusponi, M. Veronese, S. S. Dhesi, C. Grazioli, A. Dallmeyer, I. Cabria, R. Zeller, P. H. Dederichs, K. Kern, C. Carbone, and H. Brune, Science **300**, 1130 (2003).
[13] J. Bansmann, S. H. Baker, C. Binns, J. A. Blackman, J.-P. Bucher, J. Dorantes-Dávila, V. Dupuis, L. Favre, D. Kechrakos, A. Kleibert, K.-H. Meiwes-Broer, G. M. Pastor, A. Perez, O. Toulemonde, K. N. Trohidou, J. Tuaillon, and Y. Xie, Surf. Sci. Rep. **56**, 189 (2005).
[14] X. Xu, S. Yin, R. Moro, and W. A. de Heer, Phys. Rev. Lett. **95**,

237209 (2005).
[15] S. Yin, R. Moro, X. Xu, and W. A. de Heer, Phys. Rev. Lett. **98**, 113401 (2007).
[16] M. E. Gruner, G. Rollmann, P. Entel, and M. Farle, Phys. Rev. Lett. **100**, 087203 (2008).
[17] See, for instance, G. M. Pastor in *Atomic Clusters and Nanoparticles*, Lectures Notes of the Les Houches Summer School of Theoretical Physics, edited by C. Guet, P. Hobza, F. Spiegelman, and F. David (EDP Sciences, Les Ulis/Springer, Berlin, 2001), p. 335.
[18] K. Lee, J. Callaway, and S. Dhar, Phys. Rev. B **30**, 1724 (1984); K. Lee, J. Callaway, K. Kwong, R. Tang and A. Ziegler, *ibid.* **31**, 1796 (1985); K. Lee and J. Callaway, *ibid.* **48**, 15358 (1993).
[19] G. M. Pastor, J. Dorantes-Dávila, and K. H. Bennemann, Physica B & C **149**, 22 (1988); Phys. Rev. B **40**, 7642 (1989).
[20] M. Castro, Ch. Jamorski, and D. Salahub, Chem. Phys. Lett. **271**, 133 (1997); B. V. Reddy, S. K. Nayak, S. N. Khanna, B. K. Rao, and P. Jena, J. Phys. Chem. A **102**, 1748 (1998).
[21] O. Diéguez, M. M. G. Alemany, C. Rey, P. Ordejón, and L. J. Gallego, Phys. Rev. B **63**, 205407 (2001).
[22] R. A. Guirado-López, J. Dorantes-Dávila, and G. M. Pastor, Phys. Rev. Lett. **90**, 226402 (2003).
[23] G. M. Pastor, J. Dorantes-Dávila, S. Pick, and H. Dreyssé, Phys. Rev. Lett. **75**, 326 (1995).
[24] G. Rollmann, M. E. Gruner, A. Hucht, R. Meyer, P. Entel, M. L. Tiago, and J. R. Chelikowsky, Phys. Rev. Lett. **99**, 083402 (2007).
[25] G. M. Pastor, J. Dorantes-Dávila, and K. H. Bennemann, Phys. Rev. B **70**, 064420 (2004).
[26] A. N. Andriotis, Z. G. Fthenakis, and M. Menon, Europhys. Lett. **76**, 1088 (2006); S. Polesya, O. Sipr, S. Bornemann, J. Minár, and H. Ebert, *ibid.* **74**, 1074 (2006).
[27] G. M. Pastor, R. Hirsch, and B. Mühlschlegel, Phys. Rev. Lett. **72**, 3879 (1994); G. M. Pastor, R. Hirsch, and B. Mühlschlegel, Phys. Rev. B **53**, 10382 (1996); F. López-Urías and G. M. Pastor, *ibid.* **59**, 5223 (1999).
[28] F. López-Urías, G. M. Pastor, and K. H. Bennemann, J. Appl. Phys. **87**, 4909 (2000); F. López-Urías and G. M. Pastor, J. Magn. Magn. Mater. **294**, e27 (2005).
[29] Yang Jinlong, F. Toigo, and W. Kelin, Phys. Rev. B **50**, 7915 (1994); Yang Jinlong, F. Toigo, Wang Kelin, and Zhang Manhong, *ibid.* **50**, 7173 (1994); K. Wildberger, V. S. Stepanyuk, P. Lang, R. Zeller, and P. H. Dederichs, Phys. Rev. Lett. **75**, 509 (1995); Saroj K. Nayak, S. E. Weber, P. Jena, K. Wildberger, R. Zeller, P. H. Dederichs, V. S. Stepanyuk, and W. Hergert, Phys. Rev. B **56**, 8849 (1997); P. Villaseñor-González, J. Dorantes-Dávila, H. Dreyssé, and G. M. Pastor, *ibid.* **55**, 15084 (1997).
[30] J. Dorantes-Dávila, G. M. Pastor and K. H. Bennemann, Solid State Commun. **59**, 159 (1986); **60**, 465 (1986).
[31] R. Garibay-Alonso, J. Dorantes-Dávila, and G. M. Pastor, Phys. Rev. B **73**, 224429 (2006).
[32] J. Hubbard, Phys. Rev. B **19**, 2626 (1979); **20**, 4584 (1979); H. Hasegawa, J. Phys. Soc. Jpn. **49**, 178 (1980); **49**, 963 (1980).
[33] Y. Kakehashi, J. Phys. Soc. Jpn. **50**, 2251 (1981).
[34] *Electron Correlation and Magnetism in Narrow-Band Systems*, Springer Series in Solid State Sciences, edited by T. Moriya (Springer, Heidelberg, 1981), Vol. 29; D. Vollhardt *et al.*, *Advances in Solid State Physics* (Vieweg, Wiesbaden, 1999), Vol. 38, p. 383.
[35] G. M. Pastor, Ph.D. thesis, Freie Universität Berlin, 1989.
[36] G. M. Pastor and J. Dorantes-Dávila, Phys. Rev. B **52**, 13799 (1995).
[37] For the sake of clarity, a *hat* ($\hat{}$) is used to distinguish operators from numbers.
[38] J. C. Slater, *Quantum Theory of Atomic Structure* (McGraw-Hill, New York, 1960), Vols. 1 and 2.
[39] J. B. Mann, Los Alamos Science Laboratory Report No. LA-3690, 1967 (unpublished).
[40] B. Mühlschlegel, Z. Phys. **208**, 94 (1968).
[41] Recent applications of the mean-field approach to TM clusters and nanostructures at $T=0$ may be found, for example, in Refs. 22 and 42, and in references therein.
[42] G. Nicolas, J. Dorantes-Dávila, and G. M. Pastor, Phys. Rev. B **74**, 014415 (2006); M. Muñoz-Navia, J. Dorantes-Dávila, D. Zitoun, C. Amiens, B. Chaudret, M.-J. Casanove, P. Lecante, N. Jaouen, A. Rogalev, M. Respaud, and G. M. Pastor, Faraday Discuss. **138**, 181 (2008).
[43] *A Guide to Monte Carlo Simulations in Statistical Physica*, 2nd ed., edited by David P. Landau and Kurt Binder (Cambridge University Press, Cambridge, 2005).
[44] R. Haydock, in *Solid State Physics*, edited by H. Ehreinreich, F. Seitz, and D. Turnbull (Academic, New York, 1980), Vol. 35, p. 215.
[45] M. E. J. Newman and G. T. Barkema, *Monte Carlo Methods in Statistical Physics* (Oxford University Press, Oxford, 1999).
[46] R. H. Swendsen and J. S. Wang, Phys. Rev. Lett. **58**, 86 (1987).
[47] U. Wolff, Phys. Rev. Lett. **62**, 361 (1989).
[48] B. A. Berg and T. Neuhaus, Phys. Lett. B **267**, 249 (1991).
[49] B. A. Berg and T. Neuhaus, Phys. Rev. Lett. **68**, 9 (1992).
[50] E. Marinari and G. Parisi, Europhys. Lett. **19**, 451 (1992).
[51] K. Hukushima and K. Nemoto, J. Phys. Soc. Jpn. **65**, 1604 (1996).
[52] As in an N-step random walk the root-mean-square average of the total magnetic moment per atom of a cluster having N uncorrelated local moments of size μ_0 is $\mu_0/\sqrt{N}$.
[53] K. Binder, R. Rauch, and V. Wildpaner, J. Phys. Chem. Solids **31**, 391 (1970).
[54] V. Korenman and R. E. Prange, Phys. Rev. Lett. **53**, 186 (1984).
[55] E. M. Haines, R. Clauberg, and R. Feder, Phys. Rev. Lett. **54**, 932 (1985).
[56] J. Guevara, F. Parisi, A. M. Llois, and M. Weissmann, Phys. Rev. B **55**, 13283 (1997); A. Vega, J. Dorantes-Dávila, L. C. Balbás, and G. M. Pastor, *ibid.* **47**, 4742 (1993); A. V. Postnikov, P. Entel, and J. M. Soler, Eur. Phys. J. D **25**, 261 (2003); O. Sipr, M. Kosuth, and H. Ebert, Phys. Rev. B **70**, 174423 (2004).
[57] F. López-Urías and G. M. Pastor, Eur. Phys. J. D **52**, 159 (2009).
[58] V. Heine, Phys. Rev. **153**, 673 (1967); W. A. Harrison, Phys. Rev. B **27**, 3592 (1983); V. L. Moruzzi and P. M. Marcus, *ibid.* **38**, 1613 (1988).
[59] From Fig. 7 it is possible to infer the distance dependence of cluster Curie $T_C(N)$. Despite changes as a function of size and structure, $T_C(N)$ always remains of the same order of magnitude as in the bulk. The actual value of T_C is the result of an interplay between two effects directly related to the reduction of the coordination numbers: the enhancement of local magnetic moments and the reduction in the number of NN couplings. For some clusters, this may lead to incidental compensations and to values of $T_C(N)$ close to the bulk one. However, in most cases one of the contributions dominates over the other (see Fig. 7).